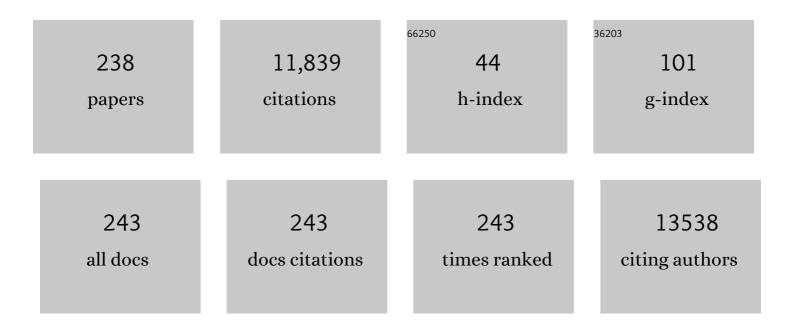
Richard Frayne

List of Publications by Year in descending order

Source: https://exaly.com/author-pdf/7352066/publications.pdf Version: 2024-02-01



#	Article	IF	CITATIONS
1	Cerebrovascular Reactivity Across the Entire Brain in Cerebral Amyloid Angiopathy. Neurology, 2022, 98, .	1.5	14
2	Distinct patterns of progressive gray and white matter degeneration in amyotrophic lateral sclerosis. Human Brain Mapping, 2022, 43, 1519-1534.	1.9	7
3	Lifespan Volume Trajectories From Non–harmonized T1–Weighted MRI Do Not Differ After Site Correction Based on Traveling Human Phantoms. Frontiers in Neurology, 2022, 13, .	1.1	4
4	Functional alterations in large-scale resting-state networks of amyotrophic lateral sclerosis: A multi-site study across Canada and the United States. PLoS ONE, 2022, 17, e0269154.	1.1	8
5	Neuroanatomical associations of the Edinburgh cognitive and Behavioural ALS screen (ECAS). Brain Imaging and Behavior, 2021, 15, 1641-1654.	1.1	11
6	Hippocampal atrophy and cognitive function in transient ischemic attack and minor stroke patients over three years. Cerebral Circulation - Cognition and Behavior, 2021, 2, 100019.	0.4	2
7	Vascular Contributions to Neurodegeneration: Protocol of the COMPASS-ND Study. Canadian Journal of Neurological Sciences, 2021, , 1-8.	0.3	6
8	Sparse precontrast T ₁ mapping for highâ€resolution wholeâ€brain DCEâ€MRI. Magnetic Resonance in Medicine, 2021, 86, 2234-2249.	1.9	3
9	Progressive Neurochemical Abnormalities in Cognitive and Motor Subgroups of Amyotrophic Lateral Sclerosis. Neurology, 2021, 97, e803-e813.	1.5	12
10	Pseudo Test-Retest Evaluation of Millimeter-Resolution Whole-Brain Dynamic Contrast-enhanced MRI in Patients with High-Grade Glioma. Radiology, 2021, 300, 410-420.	3.6	2
11	Extraction of a vascular function for a fully automated dynamic contrastâ€enhanced magnetic resonance brain image processing pipeline. Magnetic Resonance in Medicine, 2021, , .	1.9	1
12	Cerebral Amyloid Angiopathy Is Associated With Emotional Dysregulation, Impulse Dyscontrol, and Apathy. Journal of the American Heart Association, 2021, 10, e022089.	1.6	9
13	Deep Learning in Large and Multi-Site Structural Brain MR Imaging Datasets. Frontiers in Neuroinformatics, 2021, 15, 805669.	1.3	19
14	Amyloidâ€independent vascular contributions to cortical atrophy and cognition in a multiâ€center mixed cohort with low to severe small vessel disease. Alzheimer's and Dementia, 2021, 17, .	0.4	1
15	Supervised domain adaptation approach on heterogenous, multi-center MR imaging datasets. , 2021, , .		0
16	Restoration of Lossy JPEC-Compressed Brain MR Images Using Cross-Domain Neural Networks. IEEE Signal Processing Letters, 2020, 27, 141-145.	2.1	10
17	Involvement of the dentate nucleus in the pathophysiology of amyotrophic lateral sclerosis: A multi-center and multi-modal neuroimaging study. NeuroImage: Clinical, 2020, 28, 102385.	1.4	25
18	Cerebral atrophy in amyotrophic lateral sclerosis parallels the pathological distribution of TDP43. Brain Communications, 2020, 2, fcaa061.	1.5	22

#	Article	IF	CITATIONS
19	A prospective harmonized multicenter DTI study of cerebral white matter degeneration in ALS. Neurology, 2020, 95, e943-e952.	1.5	45
20	The Use of Random Forests to Identify Brain Regions on Amyloid and FDG PET Associated With MoCA Score. Clinical Nuclear Medicine, 2020, 45, 427-433.	0.7	12
21	Calgary Normative Study: design of a prospective longitudinal study to characterise potential quantitative MR biomarkers of neurodegeneration over the adult lifespan. BMJ Open, 2020, 10, e038120.	0.8	9
22	Detecting Alzheimer's Disease based on Structural Region Analysis using a 3D Shape Descriptor. , 2020, , .		2
23	Trial of remote ischaemic preconditioning in vascular cognitive impairment (TRIC-VCI): protocol. BMJ Open, 2020, 10, e040466.	0.8	7
24	Cross-sectional and longitudinal differences in peak skeletonized white matter mean diffusivity in cerebral amyloid angiopathy. NeuroImage: Clinical, 2020, 27, 102280.	1.4	25
25	Dual-domain cascade of U-nets for multi-channel magnetic resonance image reconstruction. Magnetic Resonance Imaging, 2020, 71, 140-153.	1.0	28
26	Age-related differences in cerebral blood flow and cortical thickness with an application to age prediction. Neurobiology of Aging, 2020, 95, 131-142.	1.5	14
27	Enhanced Deep-Learning-Based Magnetic Resonance Image Reconstruction by Leveraging Prior Subject-Specific Brain Imaging: Proof-of-Concept Using a Cohort of Presumed Normal Subjects. IEEE Journal on Selected Topics in Signal Processing, 2020, 14, 1126-1136.	7.3	12
28	Cerebrovascular reactivity in cerebral amyloid angiopathy, Alzheimer disease, and mild cognitive impairment. Neurology, 2020, 95, e1333-e1340.	1.5	18
29	High-resolution T2-FLAIR and non-contrast CT brain atlas of the elderly. Scientific Data, 2020, 7, 56.	2.4	20
30	Efficacy and safety of nerinetide for the treatment of acute ischaemic stroke (ESCAPE-NA1): a multicentre, double-blind, randomised controlled trial. Lancet, The, 2020, 395, 878-887.	6.3	400
31	White matter tract microstructure and cognitive performance after transient ischemic attack. PLoS ONE, 2020, 15, e0239116.	1.1	9
32	Interdatabase Variability in Cortical Thickness Measurements. Cerebral Cortex, 2019, 29, 3282-3293.	1.6	5
33	Convolutional neural networks for skull-stripping in brain MR imaging using silver standard masks. Artificial Intelligence in Medicine, 2019, 98, 48-58.	3.8	33
34	Non-Binary Approaches for Classification of Amyloid Brain PET. , 2019, , .		0
35	Automatic identification of atherosclerosis subjects in a heterogeneous MR brain imaging data set. Magnetic Resonance Imaging, 2019, 62, 18-27.	1.0	10
36	Cerebral degeneration in amyotrophic lateral sclerosis. Neurology: Clinical Practice, 2019, 9, 400-407.	0.8	13

#	Article	IF	CITATIONS
37	Investigation of Fully Connected Neural Networks for Reconstruction of MR Images. IFMBE Proceedings, 2019, , 293-298.	0.2	Ο
38	Quantifying bloodâ€brain barrier leakage in small vessel disease: Review and consensus recommendations. Alzheimer's and Dementia, 2019, 15, 840-858.	0.4	134
39	Longitudinal Brain Atrophy Rates in Transient Ischemic Attack and Minor Ischemic Stroke Patients and Cognitive Profiles. Frontiers in Neurology, 2019, 10, 18.	1.1	15
40	Harmonizing brain magnetic resonance imaging methods for vascular contributions to neurodegeneration. Alzheimer's and Dementia: Diagnosis, Assessment and Disease Monitoring, 2019, 11, 191-204.	1.2	65
41	Brain Extraction Network Trained with "Silver Standard" Data and Fine-Tuned with Manual Annotation for Improved Segmentation. , 2019, , .		Ο
42	A Hybrid Frequency-Domain/Image-Domain Deep Network for Magnetic Resonance Image Reconstruction. , 2019, , .		28
43	The Use of Random Forests to Classify Amyloid Brain PET. Clinical Nuclear Medicine, 2019, 44, 784-788.	0.7	15
44	Diffusion-weighted imaging lesion growth occurs despite recanalization in acute ischemic stroke: Implications for future treatment trials. International Journal of Stroke, 2019, 14, 257-264.	2.9	15
45	Quality Control Framework for Large MR Datasets: Automated Approaches to Outlier Detection. IFMBE Proceedings, 2019, , 387-391.	0.2	0
46	Common Carotid Artery Lumen Automatic Segmentation from Cine Fast Spin Echo Magnetic Resonance Imaging. Lecture Notes in Computer Science, 2019, , 16-24.	1.0	0
47	Abstract WP567: The Association Between Decreased Cerebral Blood Flow in Transient Ischemic Attack Patients and Cognition. Stroke, 2019, 50, .	1.0	Ο
48	Reliability of computer-aided diagnosis tools with multi-center MR datasets: impact of training protocol. , 2019, , .		0
49	Oculomotor Cognitive Control Abnormalities in Australian Rules Football Players with a History of Concussion. Journal of Neurotrauma, 2018, 35, 730-738.	1.7	29
50	An open, multi-vendor, multi-field-strength brain MR dataset and analysis of publicly available skull stripping methods agreement. NeuroImage, 2018, 170, 482-494.	2.1	131
51	Multicenter Imaging Studies: Automated Approach to Evaluating Data Variability and the Role of Outliers. , 2018, , .		1
52	Silver standard masks for data augmentation applied to deep-learning-based skull-stripping. , 2018, , .		11
53	Normal Brain Aging: Prediction of Age, Sex and White Matter Hyperintensities Using a MR Image-Based Machine Learning Technique. Lecture Notes in Computer Science, 2018, , 538-545.	1.0	3
54	Cortical Microinfarcts on 3T Magnetic Resonance Imaging in Cerebral Amyloid Angiopathy. Stroke, 2018, 49, 1899-1905.	1.0	22

#	Article	IF	CITATIONS
55	A longitudinal magnetic resonance imaging study of neurodegenerative and small vessel disease, and clinical cognitive trajectories in non demented patients with transient ischemic attack: the PREVENT study. BMC Geriatrics, 2018, 18, 163.	1.1	13
56	Reliability of using single specialist annotation for designing and evaluating automatic segmentation methods: A skull stripping case study. , 2018, , .		1
57	WMH Segmentation Challenge: AÂTexture-Based Classification Approach. Lecture Notes in Computer Science, 2018, , 489-500.	1.0	4
58	Abstract TP417: Cortical Microinfarcts on 3T MRI in Cerebral Amyloid Angiopathy: Associations With MRI Burden and Cognitive Dysfunction. Stroke, 2018, 49, .	1.0	0
59	Quantitative susceptibility mapping at 3 T: comparison of acquisition methodologies. NMR in Biomedicine, 2017, 30, e3492.	1.6	11
60	Identification of neurovascular changes associated with cerebral amyloid angiopathy from subject-specific hemodynamic response functions. Journal of Cerebral Blood Flow and Metabolism, 2017, 37, 3433-3445.	2.4	14
61	Functional magnetic resonance imaging responses in CADASIL. Journal of the Neurological Sciences, 2017, 375, 248-254.	0.3	11
62	Therapeutic Strategies and Drug Development for Vascular Cognitive Impairment. Journal of the American Heart Association, 2017, 6, .	1.6	39
63	MR imaging of carotid webs. Neuroradiology, 2017, 59, 361-365.	1.1	41
64	[P3–012]: OUTCOMES IN VASCULAR DEMENTIA TRIAL PATIENTS: A METAâ€ANALYSIS OF PLACEBO DATA FROM PRIOR RANDOMIZED CONTROLLED TRIALS. Alzheimer's and Dementia, 2017, 13, P933.	M _{0.4}	0
65	Common Carotid Artery Lumen Segmentation from Cardiac Cycle-Resolved Cine Fast Spin Echo Magnetic Resonance Imaging. , 2017, , .		0
66	White Matter Structural Connectivity Is Not Correlated to Cortical Resting-State Functional Connectivity over the Healthy Adult Lifespan. Frontiers in Aging Neuroscience, 2017, 9, 144.	1.7	51
67	Probabilistic Segmentation of Brain White Matter Lesions Using Texture-Based Classification. Lecture Notes in Computer Science, 2017, , 71-78.	1.0	3
68	Abstract WP442: Diffusion Tensor Imaging of White Matter Tracts in Transient Ischemic Attack Patients. Stroke, 2017, 48, .	1.0	0
69	Multislice <i>T</i> ₁ -prepared 2D single-shot EPI: analysis of a clinical <i>T</i> ₁ mapping method unbiased by <i>B</i> ₀ or <i>B</i> ₁ inhomogeneity. NMR in Biomedicine, 2016, 29, 1056-1069.	1.6	4
70	P2â€027: Systematic Review of RCTS of Interventions for Vascular Cognitive Impairment. Alzheimer's and Dementia, 2016, 12, P619.	0.4	0
71	Longitudinal decrease in blood oxygenation level dependent response in cerebral amyloid angiopathy. NeuroImage: Clinical, 2016, 11, 461-467.	1.4	24
72	3D texture-based classification applied on brain white matter lesions on MR images. Proceedings of SPIE, 2016	0.8	2

#	Article	IF	CITATIONS
73	METACOHORTS for the study of vascular disease and its contribution to cognitive decline and neurodegeneration: An initiative of the Joint Programme for Neurodegenerative Disease Research. Alzheimer's and Dementia, 2016, 12, 1235-1249.	0.4	82
74	Flow and pressure measurements in aneurysms and arteriovenous malformations with phase contrast MR imaging. Magnetic Resonance Imaging, 2016, 34, 1322-1328.	1.0	12
75	Quantitative Perfusion and Permeability Biomarkers in Brain Cancer from Tomographic CT and MR Images. Biomarkers in Cancer, 2016, 8s2, BIC.S31801.	3.6	11
76	Application of a Novel Measure of In Vivo Knee Joint Laxity. Journal of Biomechanical Engineering, 2016, 138, .	0.6	3
77	Cerebral Amyloid Angiopathy Is Associated With Executive Dysfunction and Mild Cognitive Impairment. Stroke, 2016, 47, 2010-2016.	1.0	90
78	Phase Error Correction in Time-Averaged 3D Phase Contrast Magnetic Resonance Imaging of the Cerebral Vasculature. PLoS ONE, 2016, 11, e0149930.	1.1	8
79	Cerebrovascular MRI: a review of stateâ€ofâ€theâ€art approaches, methods and techniques. NMR in Biomedicine, 2015, 28, 767-791.	1.6	38
80	Fast spin echo imaging of carotid artery dynamics. Magnetic Resonance in Medicine, 2015, 74, 1103-1109.	1.9	9
81	Phase contrast MR imaging measurements of blood flow in healthy human cerebral vessel segments. Physiological Measurement, 2015, 36, 1517-1527.	1.2	31
82	Final infarct volume estimation on 1-week follow-up MR imaging is feasible and is dependent on recanalization status. NeuroImage: Clinical, 2015, 7, 1-6.	1.4	28
83	Reduced Blood Flow in Normal White Matter Predicts Development of Leukoaraiosis. Journal of Cerebral Blood Flow and Metabolism, 2015, 35, 1610-1615.	2.4	90
84	A systematic literature review of the effect of carotid atherosclerosis on local vessel stiffness and elasticity. Atherosclerosis, 2015, 243, 211-222.	0.4	75
85	Time-Dependent Computed Tomographic Perfusion Thresholds for Patients With Acute Ischemic Stroke, 2015, 46, 3390-3397.	1.0	114
86	Early cerebral small vessel disease and brain volume, cognition, and gait. Annals of Neurology, 2015, 77, 251-261.	2.8	150
87	Hemodynamic alterations measured with phase-contrast MRI in a giant cerebral aneurysm treated with a flow-diverting stent. Radiology Case Reports, 2015, 10, 1109.	0.2	10
88	Reliability of neuroanatomical measurements in a multisite longitudinal study of youth at risk for psychosis. Human Brain Mapping, 2014, 35, 2424-2434.	1.9	76
89	Incidental Magnetic Resonance Diffusion-Weighted Imaging–Positive Lesions Are Rare in Neurologically Asymptomatic Community-Dwelling Adults. Stroke, 2014, 45, 2115-2117.	1.0	24
90	Validity of the diagnostic criteria for chronic cerebrospinal venous insufficiency and association with multiple sclerosis. Cmaj, 2014, 186, E418-E426.	0.9	12

#	Article	IF	CITATIONS
91	ENHANCING DELIVERY OF GADOLINIUM-LOADED, TARGETED NANOPARTICLES: EFFECT OF STERIC HINDRANCE ON FOLATE RECEPTOR-MEDIATED CELLULAR UPTAKE IN VITRO. Canadian Journal of Cardiology, 2014, 30, S217.	0.8	0
92	The Prevalence of Incidental Findings in Multiple Sclerosis Patients. Canadian Journal of Neurological Sciences, 2014, 41, 49-52.	0.3	2
93	Atherosclerosis Imaging and the Canadian Atherosclerosis Imaging Network. Canadian Journal of Cardiology, 2013, 29, 297-303.	0.8	25
94	Susceptibility-Weighted Imaging is More Reliable Than T2*-Weighted Gradient-Recalled Echo MRI for Detecting Microbleeds. Stroke, 2013, 44, 2782-2786.	1.0	220
95	Neuroimaging standards for research into small vessel disease and its contribution to ageing and neurodegeneration. Lancet Neurology, The, 2013, 12, 822-838.	4.9	3,919
96	A statistical method for characterizing the noise in nonlinearly reconstructed images from undersampled MR data: The POCS example. Magnetic Resonance Imaging, 2013, 31, 1587-1598.	1.0	4
97	Accelerated passive MR catheter tracking into the carotid artery of canines. Magnetic Resonance Imaging, 2013, 31, 120-129.	1.0	5
98	An application of algebraic method on MR T2 imaging of knee articular cartilage. , 2013, , .		0
99	Neurovascular decoupling is associated with severity of cerebral amyloid angiopathy. Neurology, 2013, 81, 1659-1665.	1.5	118
100	The Knee Loading Apparatus: Axial, Anterior, and Compressive Loading With Magnetic Resonance Imaging. Journal of Mechanical Design, Transactions of the ASME, 2013, 135, .	1.7	7
101	Semiautomated Multimodal Breast Image Registration. International Journal of Biomedical Imaging, 2012, 2012, 1-14.	3.0	4
102	Using X-Ray Mammograms to Assist in Microwave Breast Image Interpretation. International Journal of Biomedical Imaging, 2012, 2012, 1-11.	3.0	5
103	Cavitation After Acute Symptomatic Lacunar Stroke Depends on Time, Location, and MRI Sequence. Stroke, 2012, 43, 1837-1842.	1.0	92
104	Planimetric Hematoma Measurement in Patients With Intraventricular Hemorrhage. Stroke, 2012, 43, 1961-1963.	1.0	27
105	Voxel-based relaxometry for cases of an unresolved epilepsy diagnosis. Epilepsy Research, 2012, 99, 46-54.	0.8	4
106	Algebraic T2 estimation improves detection of right temporal lobe epilepsy by MR T2 relaxometry. NeuroImage, 2011, 58, 189-197.	2.1	13
107	A human cell model for dynamic testing of MR contrast agents. BioTechniques, 2011, 50, 120-123.	0.8	1
108	Quantomo: Validation of a Computer-Assisted Methodology for the Volumetric Analysis of Intracerebral Haemorrhage. International Journal of Stroke, 2011, 6, 302-305.	2.9	73

#	Article	lF	CITATIONS
109	Stroke on awakening and the tissue window for thrombolysis. Lancet Neurology, The, 2011, 10, 951-952.	4.9	1
110	Deconvolution with simple extrapolation for improved cerebral blood flow measurement in dynamic susceptibility contrast magnetic resonance imaging during acute ischemic stroke. Magnetic Resonance Imaging, 2011, 29, 620-629.	1.0	10
111	Dynamic phantom with heart, lung, and blood motion for initial validation of MRI techniques. Journal of Magnetic Resonance Imaging, 2011, 34, 941-946.	1.9	14
112	Hippocampal T2 abnormalities in healthy adults. Epilepsy Research, 2011, 95, 273-276.	0.8	1
113	SU-E-I-129: Determining the Cramer-Rao Lower Bound in Magnetic Resonance Imaging. Medical Physics, 2011, 38, 3425-3425.	1.6	0
114	Perfusion parameters derived from bolusâ€ŧracking perfusion imaging are immune to tracer recirculation. Journal of Magnetic Resonance Imaging, 2010, 31, 753-756.	1.9	9
115	A simulationâ€based analysis of the potential of compressed sensing for accelerating passive mr catheter visualization in endovascular therapy. Magnetic Resonance in Medicine, 2010, 63, 473-483.	1.9	9
116	Age effects on voxel-based relaxometry used for epileptic patients. Epilepsy Research, 2010, 92, 41-47.	0.8	3
117	Fluid Attenuated Inversion Recovery (FLAIR) Imaging of the Normal Brain: Comparisons between Under the Conditions of 3.0 Tesla and 1.5 Tesla. Korean Journal of Radiology, 2010, 11, 19.	1.5	9
118	Less could be more when it comes to diffusion imaging of acute stroke. Neurology, 2010, 74, 1936-1937.	1.5	2
119	Atlas-Based Topographical Scoring for Magnetic Resonance Imaging of Acute Stroke. Stroke, 2010, 41, 455-460.	1.0	18
120	A General Description of Linear Time-Frequency Transforms and Formulation of a Fast, Invertible Transform That Samples the Continuous S-Transform Spectrum Nonredundantly. IEEE Transactions on Signal Processing, 2010, 58, 281-290.	3.2	118
121	A tutorial on the precessional behaviour of hydrogen nuclei in external magnetic fields. Canadian Journal of Physics, 2010, 88, 465-477.	0.4	0
122	Analysis Techniques for Congruence of the Patellofemoral Joint. Journal of Biomechanical Engineering, 2009, 131, 124503.	0.6	16
123	Analytical characterization of RF phaseâ€cycled balanced steadyâ€state free precession. Concepts in Magnetic Resonance Part A: Bridging Education and Research, 2009, 34A, 133-143.	0.2	24
124	Cerebral blood flow estimation in vivo using local tissue reference functions. Journal of Magnetic Resonance Imaging, 2009, 29, 183-188.	1.9	5
125	Evolution of hyperacute stroke over 6 hours using serial MR perfusion and diffusion maps. Journal of Magnetic Resonance Imaging, 2009, 29, 1262-1270.	1.9	16
126	Differences in patellofemoral contact mechanics associated with patellofemoral pain syndrome. Journal of Biomechanics, 2009, 42, 2802-2807.	0.9	46

#	Article	IF	CITATIONS
127	Single-subject voxel-based relaxometry for clinical assessment of temporal lobe epilepsy. Epilepsy Research, 2009, 86, 23-31.	0.8	12
128	Diffusion and Perfusion MR Imaging of Acute Ischemic Stroke. Magnetic Resonance Imaging Clinics of North America, 2009, 17, 291-313.	0.6	24
129	Applications of Molecular Imaging with MR. , 2009, , 363-393.		Ο
130	Minimum detectable difference of MR diffusion maps in acute ischemic stroke. Journal of Magnetic Resonance Imaging, 2008, 27, 629-633.	1.9	2
131	Identifying lesion growth with MR imaging in acute ischemic stroke. Journal of Magnetic Resonance Imaging, 2008, 28, 837-846.	1.9	8
132	3D nonâ€contrastâ€enhanced MR angiography with balanced steadyâ€state free precession dixon method. Magnetic Resonance in Medicine, 2008, 59, 430-433.	1.9	25
133	Rapid passive MR catheter visualization for endovascular therapy using nonsymmetric truncated k-space sampling strategies. Magnetic Resonance Imaging, 2008, 26, 293-303.	1.0	6
134	Variability of Middle Cerebral Artery Blood Flow with Hypercapnia in Women. Ultrasound in Medicine and Biology, 2008, 34, 730-740.	0.7	8
135	A fast discrete S-transform for biomedical signal processing. , 2008, 2008, 2586-9.		34
136	An Improved Scoring System for Identifying Patients at High Early Risk of Stroke and Functional Impairment after an Acute Transient Ischemic Attack or Minor Stroke. International Journal of Stroke, 2008, 3, 3-10.	2.9	110
137	Unenhanced MR Angiography of the Renal Arteries with Balanced Steady-State Free Precession Dixon Method. American Journal of Roentgenology, 2008, 191, 243-246.	1.0	18
138	A comparison of texture quantification techniques based on the Fourier and S transforms. Medical Physics, 2008, 35, 4998-5008.	1.6	20
139	Obtaining DSC MRI cerebral blood flow estimates without tissue specific errors. , 2008, , .		Ο
140	Assessment of a Novel Technique for In-Vivo Investigation of Joint Cartilage Deformation Characteristics. , 2007, , 581.		0
141	Assessment of brain aneurysms by using high-resolution magnetic resonance angiography after endovascular coil delivery. Journal of Neurosurgery, 2007, 107, 283-289.	0.9	14
142	Noninvasive imaging is improving but digital subtraction angiography remains the gold standard. Neurology, 2007, 68, 2057-2058.	1.5	17
143	Magnetization evolution in balanced steady-state free precession with continuously moving table. Physics in Medicine and Biology, 2007, 52, N173-N184.	1.6	2
144	3-Tesla versus 1.5-Tesla Magnetic Resonance Diffusion and Perfusion Imaging in Hyperacute Ischemic Stroke. Cerebrovascular Diseases, 2007, 24, 361-368.	0.8	29

#	Article	IF	CITATIONS
145	Realistic breast models for second generation tissue sensing adaptive radar system. , 2007, , .		15
146	Reexamining the quantification of perfusion MRI data in the presence of bolus dispersion. Journal of Magnetic Resonance Imaging, 2007, 25, 639-643.	1.9	16
147	PerfTool: A software platform for investigating bolus-tracking perfusion imaging quantification strategies. Journal of Magnetic Resonance Imaging, 2007, 25, 653-659.	1.9	21
148	Improved dynamic susceptibility contrast (DSC)â€MR perfusion estimates by motion correction. Journal of Magnetic Resonance Imaging, 2007, 26, 1167-1172.	1.9	19
149	MRI of ischemic stroke in canines: Applications for monitoring intraarterial thrombolysis. Journal of Magnetic Resonance Imaging, 2007, 26, 1421-1428.	1.9	12
150	Robust dynamic susceptibility contrast MR perfusion using 4D nonlinear noise filters. Journal of Magnetic Resonance Imaging, 2007, 26, 1514-1522.	1.9	20
151	Knee Joint Motion Quantified Using the Finite Helical Axis Method. , 2007, , .		Ο
152	A Novel Measure of In-Vivo Knee Joint Laxity. , 2007, , .		0
153	Stroke Imaging at 3.0 T. Neuroimaging Clinics of North America, 2006, 16, 343-366.	0.5	8
154	Control of end-tidal PCO2 reduces middle cerebral artery blood velocity variability: Implications for physiological neuroimaging. NeuroImage, 2006, 29, 1272-1277.	2.1	14
155	A new method of creating intervertebral disc disruption of various grades. Clinical Biomechanics, 2006, 21, 21-25.	0.5	7
156	Automatic Surface Matching for the Registration of LIDAR Data and MR Imagery. ETRI Journal, 2006, 28, 162-174.	1.2	15
157	Registration of knee joint surfaces for the in-vivo study of joint injuries based on magnetic resonance imaging. , 2006, 6144, 935.		1
158	MR Angiography Compared to Conventional Selective Angiography in Acute Stroke. Canadian Journal of Neurological Sciences, 2006, 33, 58-62.	0.3	35
159	Differences between middle cerebral artery blood velocity waveforms of young and postmenopausal women. Menopause, 2006, 13, 303-313.	0.8	21
160	MR image reconstruction of sparsely sampled 3D k-space data by projection-onto-convex sets. Magnetic Resonance Imaging, 2006, 24, 761-773.	1.0	15
161	A real-time 3D large field-of-view MRI system with interactive table motion. Concepts in Magnetic Resonance Part B, 2006, 29B, 28-41.	0.3	4
162	Interactive continuously moving table (iCMT) large field-of-view real-time MRI. Magnetic Resonance in Medicine, 2006, 55, 1202-1209.	1.9	8

#	Article	IF	CITATIONS
163	Passive catheter visualization in magnetic resonance–guided endovascular therapy using multicycle projection dephasers. Journal of Magnetic Resonance Imaging, 2006, 24, 160-167.	1.9	13
164	Acute Ischemic Stroke: Accuracy of Diffusion-weighted MR Imaging—Effects ofbValue and Cerebrospinal Fluid Suppression. Radiology, 2006, 238, 232-239.	3.6	22
165	Time-Efficient Breath-Hold Abdominal MRI at 3.0 T. American Journal of Roentgenology, 2006, 187, 649-657.	1.0	11
166	Is correction necessary when clinically determining quantitative cerebral perfusion parameters from multi-slice dynamic susceptibility contrast MR studies?. Physics in Medicine and Biology, 2006, 51, 407-424.	1.6	23
167	Approaches to validating the "quantity" in quantitative MR cerebral perfusion studies. , 2006, , .		2
168	Sci-Fri PM Imaging-01: Comparison of POCS and cTERA Image Reconstruction Algorithms Applied to 3D Sparsely Sampled k-Space Data. Medical Physics, 2006, 33, 2670-2670.	1.6	1
169	Sci-Fri PM Imaging-09: Robust MR-DSC Perfusion using a Patient Motion Correction Scheme. Medical Physics, 2006, 33, 2671-2671.	1.6	0
170	Sci-Fri AM General-08: Image Fusion for Catheter Tracking in MR-Guided Endovascular Therapy. Medical Physics, 2006, 33, 2669-2669.	1.6	0
171	An alternative viewpoint of the similarities and differences of SVD and FT deconvolution algorithms used for quantitative MR perfusion studies. Magnetic Resonance Imaging, 2005, 23, 481-492.	1.0	27
172	Orientation of tendons in vivo with active and passive knee muscles. Journal of Biomechanics, 2005, 38, 1780-1788.	0.9	34
173	A Novel Method to Derive Separate Gray and White Matter Cerebral Blood Flow Measures from MR Imaging of Acute Ischemic Stroke Patients. Journal of Cerebral Blood Flow and Metabolism, 2005, 25, 1236-1243.	2.4	23
174	MR Perfusion and Diffusion in Acute Ischemic Stroke: Human Gray and White Matter have Different Thresholds for Infarction. Journal of Cerebral Blood Flow and Metabolism, 2005, 25, 1280-1287.	2.4	101
175	The impact of partial-volume effects in dynamic susceptibility contrast magnetic resonance perfusion imaging. Journal of Magnetic Resonance Imaging, 2005, 22, 390-399.	1.9	45
176	Advantages of frequency-domain modeling in dynamic-susceptibility contrast magnetic resonance cerebral blood flow quantification. Magnetic Resonance in Medicine, 2005, 53, 700-707.	1.9	17
177	Imaging of the brain in acute ischaemic stroke: comparison of computed tomography and magnetic resonance diffusion-weighted imaging. Journal of Neurology, Neurosurgery and Psychiatry, 2005, 76, 1528-1533.	0.9	314
178	Reassessing the clinical efficacy of two MR quantitative DSC PWI CBF algorithms following cross-calibration with PET images. Physics in Medicine and Biology, 2005, 50, 1251-1263.	1.6	14
179	SU-EE-A4-01: Regional Change in Brain Perfusion, in Irradiated Normal Tissue: Correlation Study Between Perfusion MRI and Spatial Distribution of Radiation Dose Delivered. Medical Physics, 2005, 32, 1900-1900.	1.6	0
180	Sci-PM Thurs - 04: A comparative study between multi-station and moving-table methods with steady-state free precession. Medical Physics, 2005, 32, 2408-2408.	1.6	0

#	Article	IF	CITATIONS
181	The probability of middle cerebral artery MRA flow signal abnormality with quantified CT ischaemic change: targets for future therapeutic studies. Journal of Neurology, Neurosurgery and Psychiatry, 2004, 75, 1426-1430.	0.9	31
182	A comparison of images generated from diffusion-weighted and diffusion-tensor imaging data in hyper-acute stroke. Journal of Magnetic Resonance Imaging, 2004, 20, 193-200.	1.9	35
183	Removing the effect of SVD algorithmic artifacts present in quantitative MR perfusion studies. Magnetic Resonance in Medicine, 2004, 51, 631-634.	1.9	86
184	Fluid-attenuated inversion recovery preparation: not an improvement over conventional diffusion-weighted imaging at 3T in acute ischemic stroke. American Journal of Neuroradiology, 2004, 25, 1653-8.	1.2	13
185	Signal-to-noise ratio effects in quantitative cerebral perfusion using dynamic susceptibility contrast agents. Magnetic Resonance in Medicine, 2003, 49, 122-128.	1.9	44
186	Contrast-enhanced MR angiography of the intracranial circulation. Magnetic Resonance Imaging Clinics of North America, 2003, 11, 599-614.	0.6	29
187	Reliability of Assessing Percentage of Diffusion-Perfusion Mismatch. Stroke, 2003, 34, 1681-1683.	1.0	98
188	Space–time relationship in continuously moving table method for large FOV peripheral contrast-enhanced magnetic resonance angiography. Physics in Medicine and Biology, 2003, 48, 2739-2752.	1.6	11
189	Magnetic Resonance Imaging at 3.0 Tesla: Challenges and Advantages in Clinical Neurological Imaging. Investigative Radiology, 2003, 38, 385-402.	3.5	152
190	Title is missing!. Investigative Radiology, 2003, 38, 385-402.	3.5	44
191	Impulse noise reduction in MR images using one rule-base merging method of fuzzy weighted mean filters. , 2003, , .		0
192	Time-resolved Three-dimensional Contrast-enhanced MR Angiography of the Peripheral Vessels. Radiology, 2002, 225, 43-52.	3.6	152
		5.0	
193	Rapid generation of preview images for real-time 3D MR angiography. Physics in Medicine and Biology, 2002, 47, N17-N24.	1.6	3
193 194	Rapid generation of preview images for real-time 3D MR angiography. Physics in Medicine and Biology,		3 16
	Rapid generation of preview images for real-time 3D MR angiography. Physics in Medicine and Biology, 2002, 47, N17-N24. Microbleeding on MRI as a Marker for Hemorrhage After Stroke Thrombolysis. Stroke, 2002, 33,	1.6	
194	Rapid generation of preview images for real-time 3D MR angiography. Physics in Medicine and Biology, 2002, 47, N17-N24. Microbleeding on MRI as a Marker for Hemorrhage After Stroke Thrombolysis. Stroke, 2002, 33, 1457-1458. Validation of Injection Parameters for Catheter-Directed Intraarterial Gadolinium-Enhanced MR	1.6 1.0	16
194 195	Rapid generation of preview images for real-time 3D MR angiography. Physics in Medicine and Biology, 2002, 47, N17-N24. Microbleeding on MRI as a Marker for Hemorrhage After Stroke Thrombolysis. Stroke, 2002, 33, 1457-1458. Validation of Injection Parameters for Catheter-Directed Intraarterial Gadolinium-Enhanced MR Angiography. Academic Radiology, 2002, 9, 172-185. Acute Intravenous–Intra-Arterial Revascularization Therapy for Severe Ischemic Stroke. Stroke, 2002,	1.6 1.0 1.3	16 21

#	Article	IF	CITATIONS
199	Comparison of pre- and postcontrast 3D time-of-flight MR angiography for the evaluation of distal intracranial branch occlusions in acute ischemic stroke. American Journal of Neuroradiology, 2002, 23, 557-67.	1.2	57
200	Novel Magnetic Resonance Signal Enhancing Coating Material. Advanced Materials, 2001, 13, 490-493.	11.1	9
201	Symptomatic hemorrhage after alteplase therapy not due to silent ischemia. BMC Neurology, 2001, 1, 1.	0.8	11
202	3D MR DSA: Effects of injection protocol and image masking. Journal of Magnetic Resonance Imaging, 2000, 12, 476-487.	1.9	47
203	MR virtual colonography using hyperpolarized3He as an endoluminal contrast agent: Demonstration of feasibility. Magnetic Resonance in Medicine, 2000, 44, 813-816.	1.9	15
204	Method for rapidly determining and reconstructing the peak arterial frame from a time-resolved CE-MRA exam. Magnetic Resonance in Medicine, 2000, 44, 817-820.	1.9	18
205	Endovascular Treatment of Experimental Canine Aneurysms: Feasibility with MR Imaging Guidance. Radiology, 2000, 215, 516-519.	3.6	45
206	Real-Time MR Imaging-guided Passive Catheter Tracking with Use of Gadolinium-filled Catheters. Journal of Vascular and Interventional Radiology, 2000, 11, 1079-1085.	0.2	99
207	Determination of Optimal Injection Parameters for Intraarterial Gadolinium-enhanced MR Angiography. Journal of Vascular and Interventional Radiology, 2000, 11, 1277-1284.	0.2	45
208	MR-guided Angioplasty of Renal Artery Stenosis in a Pig Model: A Feasibility Study. Journal of Vascular and Interventional Radiology, 2000, 11, 373-381.	0.2	79
209	Characterization of common carotid artery blood-flow waveforms in normal human subjects. Physiological Measurement, 1999, 20, 219-240.	1.2	279
210	Design and Validation of a Motion Stage for In Vitro MR Experiments. Journal of Magnetic Resonance Imaging, 1999, 10, 972-977.	1.9	3
211	Intraarterial Gadolinium-enhanced 2D and 3D MR Angiography: A Preliminary Study. Journal of Vascular and Interventional Radiology, 1999, 10, 1315-1321.	0.2	42
212	Minimizing interference from magnetic resonance imagers during electrocardiography. IEEE Transactions on Biomedical Engineering, 1998, 45, 160-164.	2.5	48
213	A rapid 2D time-resolved variable-ratek-space sampling MR technique for passive catheter tracking during endovascular procedures. Magnetic Resonance in Medicine, 1998, 40, 356-362.	1.9	107
214	3D Time-resolved contrast-enhanced MR DSA: Advantages and tradeoffs. Magnetic Resonance in Medicine, 1998, 40, 571-581.	1.9	93
215	Contrast-enhanced 3D MR DSA of the carotid artery bifurcation: preliminary study of comparison with unenhanced 2D and 3D time-of-flight MR angiography Radiology, 1998, 208, 447-451.	3.6	106
216	Rapid measurement of Gd-DTPA extraction fraction in a dialysis system using echo-planar imaging. Medical Physics, 1997, 24, 1907-1913.	1.6	19

#	Article	IF	CITATIONS
217	Effect of and correction for in-plane myocardial motion on estimates of coronary-volume flow rates. Journal of Magnetic Resonance Imaging, 1997, 7, 815-828.	1.9	19
218	MR Angiography with Three-dimensional MR Digital Subtraction Angiography. Topics in Magnetic Resonance Imaging, 1996, 8, 366???388.	0.7	24
219	Effects of through-plane myocardial motion on phase-difference and complex-difference measurements of absolute coronary artery flow. Journal of Magnetic Resonance Imaging, 1996, 6, 113-123.	1.9	22
220	Frequency response of multi-phase segmentedk-space phase-contrast. Magnetic Resonance in Medicine, 1996, 35, 755-762.	1.9	25
221	Time-resolved contrast-enhanced 3D MR angiography. Magnetic Resonance in Medicine, 1996, 36, 345-351.	1.9	861
222	MR measurement and numerical simulation of steady flow in an end-to-side anastomosis model. Journal of Biomechanics, 1996, 29, 537-542.	0.9	23
223	Frequency response of prospectively gated phase-contrast MR velocity measurements. Journal of Magnetic Resonance Imaging, 1995, 5, 65-73.	1.9	14
224	Understanding acceleration-induced displacement artifacts in phase-contrast MR velocity measurements. Journal of Magnetic Resonance Imaging, 1995, 5, 207-215.	1.9	35
225	Accuracy of MR phase contrast velocity measurements for unsteady flow. Journal of Magnetic Resonance Imaging, 1995, 5, 428-431.	1.9	86
226	Measurement of fluid-shear rate by fourier-encoded velocity imaging. Magnetic Resonance in Medicine, 1995, 34, 378-387.	1.9	25
227	Effects of physiologic waveform variability in triggered MR imaging: Theoretical analysis. Journal of Magnetic Resonance Imaging, 1994, 4, 853-867.	1.9	21
228	Turbine flow sensor for volume-flow rate verification in MR. Magnetic Resonance in Medicine, 1994, 32, 410-417.	1.9	2
229	<title>Stenosed anthropomorphic vascular phantoms for digital subtraction angiography, magnetic resonance, and Doppler ultrasound investigations</title> . , 1994, 2163, 235.		2
230	Frequency response of retrospectively gated phase-contrast MR imaging: Effect of interpolation. Journal of Magnetic Resonance Imaging, 1993, 3, 907-917.	1.9	45
231	A geometrically accurate vascular phantom for comparative studies of x-ray, ultrasound, and magnetic resonance vascular imaging: construction and geometrical verification. Medical Physics, 1993, 20, 415-425.	1.6	55
232	Visualizing three-dimensional flow with simulated streamlines and three-dimensional phase-contrast MR imaging. Journal of Magnetic Resonance Imaging, 1992, 2, 143-153.	1.9	103
233	Computer-controlled flow simulator for MR flow studies. Journal of Magnetic Resonance Imaging, 1992, 2, 605-612.	1.9	73
234	A new strategy for imaging blood vessels in the legs using magnetic resonance (MR) imaging. , 0, , .		1

#	Article	IF	CITATIONS
235	Quantitative MR cerebral blood flow using ARMA-based deconvolution: preliminary results. , 0, , .		1
236	Matching strategy for co-registration of surfaces acquired by magnetic resonance imaging. , 0, , .		3
237	Developments in Time-Frequency Analysis of Biomedical Signals and Images Using a Generalized Fourier Synthesis. , 0, , .		0
238	Multisite Reproducibility of QSM and R ₂ * in Deep Gray Matter at 3T Using Locallyâ€Optimized Sequences in 24 Traveling Heads. NMR in Biomedicine, 0, , .	1.6	2